# Indirect Adaptive Control for Synchronous Generator: Comparison of MLP/RBF Neural Networks Approach With Lyapunov Stability Analysis

Jung-Wook Park, *Member, IEEE*, Ronald G. Harley, *Fellow, IEEE*, and
Ganesh K. Venayagamoorthy, *Senior Member, IEEE*

*Abstract*—This paper compares two indirect adaptive neurocontrollers, namely a multilayer perceptron neurocontroller (MLPNC) and a radial basis function neurocontroller (RBFNC) to control a synchronous generator. The different damping and transient performances of two neurocontrollers are compared with those of conventional linear controllers, and analyzed based on the Lyapunov direct method.

*Index Terms*—Indirect adaptive control, Lyapunov transient stability analysis, multilayer perceptron neural network (MLPN), on-line training, radial basis function neural network (RBFN), synchronous generator.

## I. INTRODUCTION

SYNCHRONOUS generator in a power system is a nonlinear, fast acting, multi-input multi-output (MIMO) device [1], [2]. Conventional linear controllers (CONVC) for the synchronous generator consist of an automatic voltage regulator (AVR) to maintain constant terminal voltage, and a speed governor to maintain constant power and constant speed at some set point. They are designed to control, in some optimal fashion, the generator around one particular operating point; and because of nonlinearities, at any other point the generator's damping performance is degraded. Artificial neural networks (NNs) offer an alternative as intelligent nonlinear adaptive controllers, called neurocontrollers.

Researchers have until now used two different types of neural networks for the neurocontrollers of generators, namely, a multilayer perceptron neural network (MLPN) [3]–[7] or a radial basis function neural network (RBFN) [8]–[12] both *in single and multimachine power system studies*. Proponents of each type of neural network (NN) have claimed advantages for their choice of NN, without comparing the performance of the other type for the same study. The applications of NNs in the power
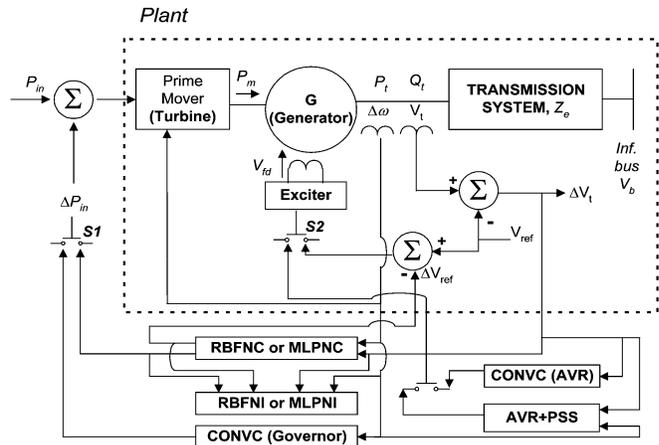
Fig. 1. Plant model used for control of a synchronous generator connected to an infinite bus.

industry are expanding, and at this stage there is no authoritative fair comparison between the MLPN and the RBFN based neurocontrollers.

This paper extends the previous work of the authors [6], [12] and makes a new contribution by directly comparing the two *continually on-line trained* neurocontrollers (MLPNC and RBFNC) (in the application of the indirect adaptive control to a synchronous generator) and analyzing different transient stability performances of the neurocontrollers based on the *Lyapunov direct method*.

## II. INDIRECT ADAPTIVE NEUROCONTROL USING BACKPROPAGATION

### A. Plant Modeling

In Fig. 1, the synchronous generator, turbine, exciter and transmission system connected to an infinite bus form the plant (dotted block in Fig. 1) that has to be controlled. Nonlinear equations are used to describe the dynamics of the plant in order to generate the data for the NN controllers and identifiers.

In the plant, $P_t$ and $Q_t$ are the real and reactive power at the generator terminals, respectively. $Z_e$ is the transmission line impedance, $P_m$ is the mechanical input power to the generator, $V_{fd}$ is the generator field voltage, $V_b$ is the infinite bus voltage, $\Delta\omega$ is the generator speed deviation, $V_t$ is the terminal voltage,
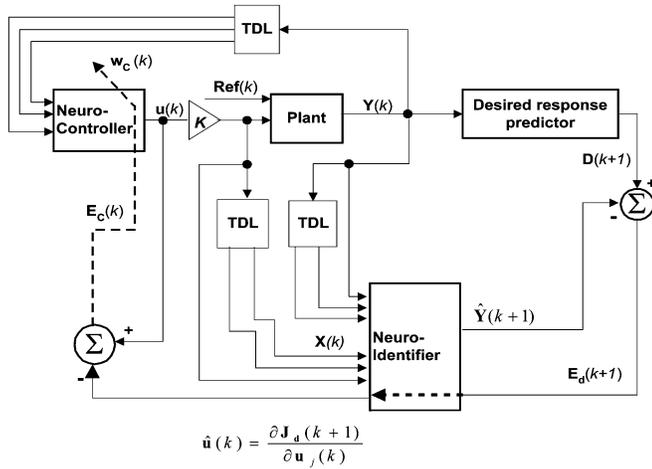
Fig. 2.  Structure of the overall system for the indirect adaptive control using a neuroidentifier and neurocontroller.

$V_{\mathrm{ref}}$ is the reference exciter voltage, and $P_{\mathrm{in}}$ is the turbine input power. The switches $S1$ and $S2$ in Fig. 1 determine the type of controllers to be used: namely the neurocontroller (RBFNC or MLPNC), or the CONVC consisting of governor and AVR. More detailed explanations are given in [6] and [12]. The exciter and turbine models used in Fig. 1 are typical [1] of those on large turbogenerators. Block diagrams and parameters of the CONVC are given in [6].

*B. Indirect Adaptive Control*

The structure of the overall system for the indirect adaptive neurocontrol [6], [12] of the plant, using the neurocontroller (RBFNC/MLPNC) and neuroidentifier (RBFNI/MLPNI), is shown in Fig. 2.

The MLPN and RBFN structures and their associated equations (used in Fig. 2 for the neuroidentifier and neurocontroller) are given in [5] and [12]. The plant input vector, $\mathbf{u}(k)$ and the plant output vector, $\mathbf{Y}(k)$ in Fig. 2 are $\mathbf{u}(k) = [\Delta V_{\mathrm{ref}}(k), \Delta P_{\mathrm{in}}(k)]$ and $\mathbf{Y}(k) = [\Delta\omega(k), \Delta V_t(k)]$ for the *on-line training* with deviation signals. The neuroidentifier's output, $\hat{\mathbf{Y}}(k+1) = \hat{f}(\mathbf{x}(k))$, where $\mathbf{x}(k) = [\mathbf{Y}(k)\mathbf{u}(k)\mathbf{Y}(k-1)\mathbf{u}(k-1)\mathbf{Y}(k-2)\mathbf{u}(k-2)]^{\mathrm{T}}$. More detailed explanations (especially for the following two issues) for the indirect adaptive control strategy are given in [6]:

- design of the desired response predictor;
- on-line training process in two phases (*precontrol phase* and *postcontrol phase*) for the neuroidentifier and neurocontroller.

Then, the estimated control signals[1] (shown in Fig. 2) $[\hat{\mathbf{u}}(k) = \partial\mathbf{J}_{\mathrm{d}}(k+1)/\partial\mathbf{u}_j(k)]$ through the neuroidentifier are

---

[1]The partial derivatives are computed through the neuroidentifier using the *backpropagation* algorithm [13], instead of the plant, to derive estimates of the dynamic derivatives of the instantaneous total least square error energy $\mathbf{J}_{\mathrm{d}}(k+1) = \sum[\mathbf{E}_{\mathrm{d}}(k+1)]^2/2$ (see Fig. 2) between the identifier's output and the predictor's output at time $k+1$, with respect to the input vector $\mathbf{u}(k)$ at time $k$. This method (based on the backpropagation algorithm) gives a direct method to compare the performances of the RBFN and MLPN because the computation of $\hat{\mathbf{u}}(k)$ requires calculating the different network Jacobians for the two NNs (MLPN and RBFN) during the real-time control of the plant [12].

expressed as follows (step-by-step derivations for (1) and (2) are given in [12]):

$$\hat{\mathbf{u}}(k)|_{\mathbf{MLPN}} = \Bigg[ \left[ f_{l,j}^1(\mathbf{g}_{l,j}(k)) \left\{ 1 - f_{l,j}^1(\mathbf{g}_{l,j}(k)) \right\} w_{l,j}(k) \right]$$
$$\times \sum_{j=1}^{m_l} \mathbf{E}_{\mathbf{d}_{L,j}}(k+1) \cdot w_{L,j}(k) \Bigg] \tag{1}$$

$$\hat{\mathbf{u}}(k)|_{\mathbf{RBFN}} = \Bigg[ \left\{ \left( 2 \sum_{p=1}^{m_l} \frac{\mathbf{C}_p - \mathbf{g}_j}{\beta_p^2} \right) f^2(\mathbf{g}_j) \right\}$$
$$\times \sum_{j=1}^{m_l} \mathbf{E}_{\mathbf{d}_{L,j}}(k+1) \cdot w_{L,j}(k) \Bigg] \tag{2}$$

where

- $L$ and $l$ denote the output layer and hidden layer, respectively;
- $j$ is the index of a particular neuron in a layer, and $m_l$ is the number of neurons in the hidden layer;
- $\mathbf{g}(k)$ is the regression vector as the activity of the neuron, and $w$ is the weights of neural networks;
- $\mathbf{C}_P$ is the $p$th center (of RBF unit) in the hidden layer of the RBFN (refer to [5] and [12]);
- The functions $f^1$ and $f^2$ are $f^1(\mathbf{x}) = 1/[1 + \exp(-\mathbf{x})]$ and $f^2(\mathbf{x}) = \exp(-\|\mathbf{x} - \mathbf{C}_j\|^2/\beta_j^2)$, respectively.

*C. Lyapunov Transient Stability Analysis*

The stability analysis of the neurocontrollers provides the information whether the controllers can allow the generator to be operated closer to its stability limit during steady state by improved damping transient performance.

Consider the following a single-machine connected to an infinite bus (SMIB) power system model. The candidate Lyapunov function $V$ (*positive-definite* around the equilibrium point) as a type of energy function and its time derivative $\dot{V}$ [14], are given as follows.

$$V = V_K + V_P + V_F = \frac{1}{2}M\Delta\omega^2 - \int_{\Delta\hat{\delta}}^{\Delta\delta} [P_m - P_e]d\delta$$
$$+ \frac{1}{2}\frac{\alpha}{\beta}(E_q' - \hat{E}_q')^2 \tag{3}$$

$$\dot{V} = -D\Delta\omega^2 - \frac{1}{T_{\mathrm{do}}'}\frac{1}{\Delta X_d}(E_q - \hat{E}_q)^2 - \frac{1}{T_{\mathrm{do}}'}\frac{1}{\Delta X_d}$$
$$\times (E_f - \hat{E}_f)(E_q - \hat{E}_q)$$
$$= -D\Delta\omega^2 - \frac{1}{T_{\mathrm{do}}'}\frac{1}{\Delta X_d}(E_q - \hat{E}_q)^2\{1 + \gamma\} \tag{4}$$

where

- The subscripts $K, P$, and $F$ refer to "kinetic," "potential," and "field," respectively;
- $M, P_m$, and $P_e$ are the inertia coefficient, mechanical power, and electrical power, respectively;
- $E_q'$ is the $q$-axis component of transient induced armature voltage;
- A "hat" above of a symbol corresponds to the postfault equilibrium point;

- $(\alpha/\beta) = (1/\Delta X_d) + B$, where $\Delta X_d = (X_d - X'_d)$, and $X_d$ and $X'_d$ are the synchronous and transient $d$-axis generator reactance, respectively. $B$ is an element of the transfer admittance matrix;
- $D$ is the damping coefficient, and $E_f$ is the excitation voltage;
- $T'_{\text{do}}$ is the open circuit armature transient time constant, and $E_q$ is the $q$-axis component of steady state induced armature voltage;
- $(E_f - \hat{E}_f) = \gamma(E_q - \hat{E}_q), \gamma > 1$.

Consequently, $\dot{V}$ in (4) is more negative when the term $(E_q - \hat{E}_q)^2$ on the right-hand side is more positive, therefore, the system can return the faster to the initial equilibrium point. In other words, *any given control improves* (*in the Lyapunov sense*) *the transient stability of the system* if it maximizes in magnitude the negative value of $\dot{V}$ at each instant of the transient state. With equations $\hat{E}_f = \hat{E}_q = E_{q,\text{ref}}$ that defines the postfault steady-state synchronous emf, the following equations can be expressed [14]:

$$E_q(t) = X_{\text{ad}} \cdot i_f(t), \quad \hat{E}_q = E_{q,\text{ref}} = X_{\text{ad}} \cdot i_{f,\text{ref}} \quad (5)$$

where $X_{\text{ad}}$ is the $d$-axis armature reaction reactance, and $i_f$ is the field current. Finally, $\dot{V}$ in (4) can be modified as follows:

$$\dot{V} = -D\Delta\omega^2 - \frac{1}{T'_{\text{do}}}\frac{1}{\Delta X_d}(1 + \gamma)X_{\text{ad}}^2(i_f(t) - i_{f,\text{ref}})^2$$
$$= -D\Delta\omega^2 - \frac{1}{T'_{\text{do}}}\frac{1}{\Delta X_d}(1 + \gamma) \cdot X_{\text{ad}}^2 \cdot \Delta i_f(t)^2$$
$$= -D\Delta\omega^2 - \frac{1}{T'_{\text{do}}}\frac{1}{\Delta X_d}(1 + \gamma) \cdot X_{\text{ad}}^2 \cdot \varepsilon \cdot \Delta V_{\text{ref}}(t)^2 \quad (6)$$

where $\Delta i_j(t)$ is the increment in the field current, and is directly determined by $\Delta V_{\text{ref}}$ (which is a controlled output from the neurocontrollers) with a proportional factor $\varepsilon$. In other words, the neurocontrollers (MLPNC/RBFNC) generate the control vector $\mathbf{u}(k) = [\Delta V_{\text{ref}}(k), \Delta P_{\text{in}}(k)]$ that follows the estimated control signal $\hat{\mathbf{u}}(k)$ in (1) and (2), thereby, affecting $\Delta V_{\text{ref}}(k)$ directly. To compare the magnitude of $\hat{\mathbf{u}}(k)$ in (1) and (2), the $\boldsymbol{O}$ notation is used to indicate "order of magnitude" for a function based on Definition 1.

*Definition 1 (Order of Magnitude):* Let $h$ and $g$ be real-valued functions. The function $h$ is $\boldsymbol{O}(g)$ as $x \to x_o$ if there is a constant $C$ (independent of $x$) such that

$$|h(x)| < C|g(x)| \quad (7)$$

for all $x$ in a neighborhood of $x_o$ or, to put it another way, if

$$\lim_{x \to x_0} \left| \frac{h(x)}{g(x)} \right| = C. \quad (8)$$

$\square$

First, the term $\sum \mathbf{E}_{\mathbf{d}_{L,j}}(k+1) \cdot w_{L,j}(k)$ in (1) and (2) has the same $\boldsymbol{O}(\cdot)$ *at the start of the transient condition* because $h(w_{L,j}(k))$ for MLPNI and RBFNI are same. The $\boldsymbol{O}(\cdot)$ of the other terms in (1) and (2) at the start of the transient condition is as follows:

- $h[f_{l,j}(\mathbf{g}_{l,j}(k))\{1 - f_{l,j}(\mathbf{g}_{l,j}(k))\}] \cong \boldsymbol{O}(10^{-1})$ and $h[w_{l,j}(k)] \cong \boldsymbol{O}(10^{-2})$,
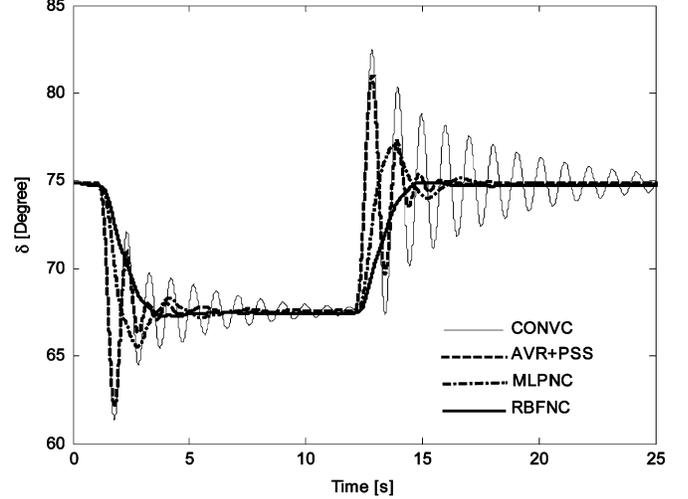


Fig. 3. Step changes in reference voltage of exciter ($P_t = 1$ pu, $Q_t = 0.234$ pu): Rotor angle ($\delta$).

- $h[f_{l,j}(\mathbf{g}_{l,j}(k))\{1 - f_{l,j}(\mathbf{g}_{l,j}(k))\}w_{l,j}(k)] \cong \boldsymbol{O}(10^{-3})$ and

$$h\left[\left(2\sum_{p=1}^{m_l}\frac{\mathbf{C}_p - \mathbf{g}_j}{\beta_p^2}\right)f(\mathbf{g}_j)\right] \cong \boldsymbol{O}(10^{-2}).$$

Consequently, the order of magnitude of $\hat{\mathbf{u}}(k)$ for the RBFNC is bigger than that for the MLPNC. This effect makes $\dot{V}$ *in* (4) *to be more negative for the RBFNC than for the MLPNC*, resulting in the better damping and faster transient responses of the RBFNC for the synchronous generator to return to its initial equilibrium point after a disturbance (shown in the next section).

## III. CASE STUDIES IN TIME-DOMAIN SIMULATION

The damping and transient performances of the neurocontrollers are now evaluated by two different types of disturbances, namely a $\pm 5\%$ step change in the exciter and a three phase short circuit at the infinite bus.

### A. $\pm 5\%$ Step Changes in the Reference Voltage of the Exciter

First, the plant is operating in a steady-state condition ($P_t = 1$ pu, $Q_t = 0.234$ pu). At $t = 1$ s, a step increase in the reference voltage of the exciter $V_{\text{ref}}$ is applied, resulting in a 5% step increase from the nominal value of the terminal voltage. At $t = 12$ s, the change in $V_{\text{ref}}$ is removed, and the system returns to the initial steady-state condition. The rotor angle ($\delta$) and terminal voltage ($V_t$) of the generator are indicators of how well the controllers are able to damp the system after this disturbance.

The results in Figs. 3 and 4 show that the neurocontrollers improve the transient system damping compared to CONVC and AVR + PSS (AVR combined with power system stabilizer (PSS): the block diagram of the PSS is shown in [15], and the selection of parameters for the PSS was made by investigating the desired steady state and transient performances depending on its objectives) in Fig. 1, and also that the RBFNC outperforms the MLPNC, i.e., the overshoot is less, and the desired point is reached faster.
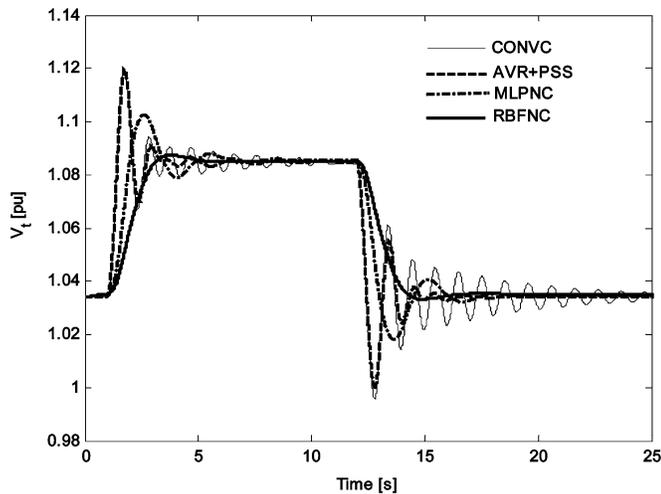
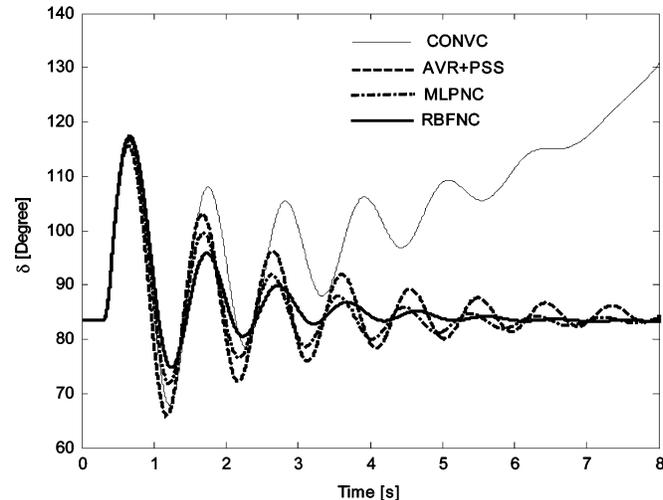Fig. 4.   Step changes in reference voltage of exciter ($P_t = 1$ pu, $Q_t = 0.234$ pu): Terminal voltage ($V_t$).



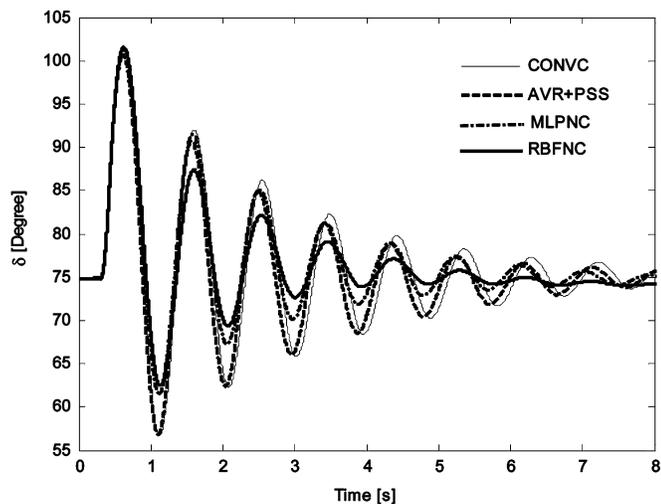Fig. 6.   Three phase short circuit test close to the stability limit ($P_t = 1.1$ pu, $Q_t = 0.19$ pu): Rotor angle ($\delta$).



Fig. 5.   Three phase short circuit test ($P_t = 1$ pu, $Q_t = 0.234$ pu): Rotor angle ($\delta$).

### B. Three Phase Short Circuit Test to Represent a Large Impulse Type Disturbance

The plant is operating at the same steady-state condition ($P_t = 1$ pu, $Q_t = 0.234$ pu). At t = 0.3 s, a temporary three phase short circuit is applied at the infinite bus for 100 ms. This test is like a severe impulse type disturbance and is used to evaluate the performance of the controllers to see if they can damp out the oscillations after the large disturbance and return the generator to its initial stable operating condition.

A comparison of the performance of the CONVC, AVR + PSS, MLPNC, and RBFNC for this test appears in Fig. 5. It shows that not only do the neurocontrollers again damp out the oscillations more effectively than the CONVC and AVR + PSS, but once again that the RBFNC provides a better damping performance than the MLPNC.

### C. Three Phase Short Circuit Test Close to the Stability Limit

The operating point is now changed to a different steady-state condition (presumably, the CONVC and AVR + PSS were not

tuned at this point) from the previous test. The active power from the generator is increased by 10% to $P_t = 1.1$ pu, and $Q_t = 0.19$ pu, which is closer to the stability limit of the generator. At t = 0.3 s, the same 100 ms three phase short circuit is again applied at the infinite bus.

The result of this test, comparing the performance of the CONVC, AVR + PSS, MLPNC, and RBFNC, is shown in Fig. 6. This result shows that the synchronous generator controlled by the CONVC goes unstable and loses synchronism after the disturbance, as indicated by the fact that the rotor angle continues to increase. In contrast though, the AVR + PSS, MLPNC and RBFNC still control the generator effectively in a stable mode. Moreover, the RBFNC once again provides a better damping performance than the MLPNC and AVR + PSS for this test. This result shows that a generator equipped with neurocontrollers can be operated at 110% power and still remain stable after such a severe fault. This has major implications on being able to operate generators (controlled by neurocontrollers) closer to their stability limits. Thermal limits may now be violated and would have to be verified in a separate study.

### IV. CONCLUSION

This paper compared the performance of a multilayer perceptron neurocontroller (MLPNC), a radial basis function neurocontroller (RBFNC), and a conventional controller (CONVC), to control a synchronous generator connected to a power system. The neurocontrollers based on the indirect adaptive control scheme use *deviation* of signals as inputs and outputs, and undergo *continually on-line training based on the backpropagation* algorithm. The different damping and transient performances of the two neurocontrollers have been analyzed using the Lyapunov direct method.

The results show that the MLPNC and RBFNC provide more damping than the CONVC and AVR + PSS. Moreover, the RBFNC is more effective than the MLPNC. The improved damping performance by the neurocontrollers allows the generator to be operated closer to its stability limit during steady state, and still remain stable after severe disturbances. The

safety margins currently observed for conventionally controlled generators can therefore be reduced by using neurocontrollers.

In general, the indirect adaptive neurocontrol method using backpropagation can be effective when the neurocontrollers are *trained on-line with deviation signals*, and the RBFN should be preferred to the MLPN.

## REFERENCES

[1] P. M. Anderson and A. A. Fouad, *Power System Control and Stability*. New York: IEEE Press, 1994, ISBN 0-7803-1029-2.

[2] B. Adkins and R. G. Harley, *The General Theory of Alternating Current Machines*. London, U.K.: Chapman and Hall, 1975, ISBN 0-412-15 560-5.

[3] P. Shamsollahi and O. P. Malik, "Direct neural adaptive control applied to synchronous generator," *IEEE Trans. Energy Conversion*, vol. 14, pp. 1341–1346, Dec. 1999.

[4] T. Kobayashi and A. Yokoyama, "An adaptive neuro-control system of synchronous generator for power system stabilization," *IEEE Trans. Energy Conv.*, vol. 11, pp. 621–630, Sept. 1996.

[5] J.-W. Park, R. G. Harley, and G. K. Venayagamoorthy, "Comparison of MLP and RBF neural networks using deviation signals for on-line identification of a synchronous generator," in *Proc. IEEE PES Winter Meeting*, vol. 1, New York, Jan. 2002, pp. 274–279.

[6] G. K. Venayagamoorthy and R. G. Harley, "A continually online trained neurocontroller for excitation and turbine control of a turbogenerator," *IEEE Trans. Energy Conv.*, vol. 16, pp. 261–269, Sept. 2001.

[7] Q. H. Wu, G. W. Irwin, and B. W. Hogg, "A neural network regulator for turbogenerators," *IEEE Trans. Neural Networks*, vol. 3, pp. 95–100, Jan. 1992.

[8] R. Segal, M. L. Kothari, and S. Madnani, "Radial basis function (RBF) network adaptive power system stabilizer," *IEEE Trans. Power Syst.*, vol. 15, pp. 722–727, May 2000.

[9] P. K. Dash, S. Mishra, and G. Panda, "A Radial basis function neural network controller for UPFC," *IEEE Trans. Power Syst.*, vol. 15, pp. 1293–1299, Nov. 2000.

[10] M. A. Abido and Y. L. Abdel-Magid, "On-line identification of synchronous machines using radial basis function neural networks," *IEEE Trans. Power Syst.*, vol. 12, pp. 1500–1506, Nov. 1997.

[11] D. Flynn, S. McLoone, G. W. Irwin, M. D. Brown, E. Swidenbank, and B. W. Hogg, "Neural control of turbogenerator systems," *Automatica*, vol. 33, no. 11, pp. 1961–1973, Nov. 1997.

[12] J.-W. Park, R. G. Harley, and G. K. Venayagamoorthy, "Comparison of MLP and RBF neural networks using deviation signals for indirect adaptive control of a synchronous generator," in *Proc. Int. Joint Conf. Neural Networks, IJCNN02*, Hawaii, May 2002, pp. 919–924.

[13] P. J. Werbos, "Backpropagation through time: What it does and how to do it," *Proc. IEEE*, vol. 78, no. 10, pp. 1550–1560, 1990.

[14] J. Machowski, S. Robak, J. W. Bialek, J. R. Bumby, and N. Abi-Samra, "Decentralized stability-enhancing control of synchronous generator," *IEEE Trans. Power Syst.*, vol. 15, no. 4, pp. 1336–1344, Nov. 2000.

[15] P. Kundur, M. Klein, G. J. Rogers, and M. S. Zywno, "Application of power system stabilizers for enhancement of overall system stability," *IEEE Trans. Power Syst.*, vol. 4, pp. 614–626, May 1989.

**Jung-Wook Park** (S'00–M'03) was born in Seoul, South Korea. He received the B.S. degree (*summa cum laude*) from Department of Electrical Engineering, Yonsei University, Seoul, South Korea, in February 1999 and the MSECE and Ph.D. degrees from the Georgia Institute of Technology, Atlanta, in December 2000 and August 2003, respectively.

He Park is now a Research Associate in the Department of Electrical and Computer Engineering, University of Wisconsin-Madison. His current research interests are in power system dynamics, electric machine, Flexible AC Transmission System (FACTS) device, hybrid system/control, optimization control algorithms, power quality, and application of artificial neural networks.

Dr. Park received the 2003 Second Prize Paper Award from the Industrial Automation and Control Committee of the IEEE Industry Applications Society (IAS).

**Ronald G. Harley** (M'77–SM'86–F'92) was born in South Africa. He received the BSc.Eng. degree (*cum laude*) and MSc.Eng. degree (*cum laude*) from the University of Pretoria, South Africa, in 1960 and 1965, respectively, and the Ph.D. degree from London University, London, U.K., in 1969.

In 1970, he was appointed to the Chair of Electrical Machines and Power Systems at the University of Natal, Durban, South Africa. He is currently the Duke Power Company Distinguished Professor at the Georgia Institute of Technology, Atlanta. His research interests are in the dynamic and transient behavior of electric machines and power systems, and controlling them by the use of power electronics and intelligent control algorithms.

Dr. Harley is a Fellow of the South African Institute of Electrical Engineers (SAIEE), the Institute of Electrical Engineers (IEE), the Royal Society in South Africa, the University of Natal, and a Founding Member of the Academy of Science in South Africa formed in 1994. He was elected as a Distinguished Lecturer by the IEEE Industry Applications Society for 2000-2001. Since 2003, he has been the Vice-President (Operations) of the IEEE Power Electronics Society.

**Ganesh K. Venayagamoorthy** (S'91–M'97–SM'02) was born in Jaffna, Sri Lanka. He received the B.Eng. (Honors) degree with a first class in electrical and electronics engineering from the Abubakar Tafawa Balewa University, Bauchi, Nigeria, in March 1994 and the M.Sc.Eng. and Ph.D. degrees in electrical engineering from the University of Natal, Durban, South Africa, in April 1999 and February 2002, respectively.

From March 1996 to April 2001, he was a Lecturer with the Durban Institute of Technology, and from May 2001 to April 2002, as a Senior Lecturer, where he lectured in Control Systems and Signal Processing among other courses. He was a Research Associate at Texas Tech University, Lubbock, in 1999 and at the University of Missouri-Rolla, from 2000 to 2001. He is currently an Assistant Professor at the University of Missouri-Rolla. His research interests are in computational intelligence, power systems, control systems and evolving hardware. He has authored over 80 papers in refereed journals and international conferences.

Dr. Venayagamoorthy is a Member of the South African Institute of Electrical Engineers (SAIEE). He is a recipient of the 2001 IEEE Neural Network Society Summer Research Scholarship, the 2003 International Neural Network Society Young Investigator Award recipient, a 2004 National Science Foundation (NSF) CAREER Award recipient and the recipient of five prize papers with the IEEE Industry Application Society and IEEE Neural Network Society. He was Technical Program Cochair of the International Joint Conference on Neural Networks (IJCNN), Portland, OR, July 20–24, 2003 and the International Conference on Intelligent Sensing and Information Processing (ICISIP), Chennai, India, January 4–7, 2004.